Immobilization of Cu and As in two contaminated soils with zero-valent iron – Long-term performance and mechanisms

Charlotta Tiberg [a,b*], Jurate Kumpiene [c], Jon Petter Gustafsson [a,d], Aleksandra Marsz [a], Ingmar Persson [e], Michel Mench [f,g], Dan B. Kleja [a,b]

[a] *Department of Soil and Environment, Swedish University of Agricultural Sciences, P. O. Box 7014, SE-750 07 Uppsala, Sweden*

[b] *Swedish Geotechnical Institute, Kornhamnstorg 61, SE-111 27 Stockholm, Sweden*

[c] *Waste Science and Technology, Luleå University of Technology, SE-971 87 Luleå, Sweden*

[d] *Division of Land and Water Resources Engineering, KTH Royal Institute of Technology, SE-100 44 Stockholm, Sweden*

[e] *Department of Chemistry and Biotechnology, Swedish University of Agricultural Sciences, P. O. Box 7015, SE-750 07 Uppsala, Sweden*

[f] *INRA, UMR 1202 BIOGECO, 69 route d'Arcachon, FR-33612, Cestas cedex, France*

[g] *University of Bordeaux, UMR 1202 BIOGECO, Bat B2, Allée Geoffroy St-Hilaire, CS50023, FR-33615 Pessac cedex, France*

* charlotta.tiberg@swedgeo.se

Abstract

Immobilization of trace elements in contaminated soils by zero-valent iron (ZVI) is a promising remediation method, but questions about its long-term performance remain unanswered. To quantify immobilization and predict possible contaminant remobilization on long timescales detailed knowledge about immobilization mechanisms is needed. This study aimed at assessing the long-term effect of ZVI amendments on dissolved copper and arsenic in contaminated soils, at exploring the immobilization mechanism(s), and at setting up a geochemical model able to estimate dissolved copper and arsenic under different scenarios. Samples from untreated and ZVI-treated plots in two field experiments where ZVI had been added 6 and 15 years ago were investigated by a combination of batch experiments, geochemical modeling and extended X-ray absorption fine structure (EXAFS) spectroscopy. Dissolved copper and arsenic concentrations were described by a multisurface geochemical model with surface complexation reactions, verified by EXAFS. The ZVI remained “reactive” after 6-15 years, i.e. the dissolved concentrations of copper and arsenic were lower in the ZVI-treated than in the untreated soils. There was a shift in copper speciation from organic matter complexes in the untreated soil to surface complexes with iron (hydr)oxides in the ZVI-treated soil. The pH value was important for copper immobilization and ZVI did not have a stabilizing effect if pH was lower than about 6. Immobilization of arsenic was slightly pH-dependent and sensitive to the competition with phosphate. If phosphate was ignored in the modeling, the dissolution of arsenate was greatly underestimated.

Keywords

copper; arsenic; ZVI; zero-valent iron; iron (hydr)oxide; immobilization; stabilization; contaminated soil; remediation; geochemical modeling; surface complexation model; EXAFS spectroscopy; X-ray absorption spectroscopy

1. Introduction

A variety of remediation methods is required to provide efficient and sustainable treatment of contaminated soils, because differences in contaminant source, soil properties, location of contaminant, land end use, etc. influence the choice of remediation methods (Cundy et al., 2013). Immobilization, or stabilization, techniques can be used to reduce excessive exposure of humans and terrestrial organisms to inorganic contaminants (Bolan et al., 2014). These techniques are mostly used at moderately contaminated sites, either singly or in combination with other remediation methods, for example as part of Gentle soil Remediation Options, (GRO) (Cundy et al., 2013). Immobilizing agents are generally mixed into the soil and the contaminants are bound through adsorption or precipitation. Although the total concentration of contaminants remains unaltered, the pollutant linkages and consequently environmental and health risks are reduced due to decreased contaminant mobility and bioavailability (Kidd et al., 2015).

One potentially effective immobilizing agent for inorganic contaminants is zero-valent iron (ZVI), in the form of iron grit (Kumpiene et al., 2006). In soils, ZVI will be rapidly transformed to reactive iron (hydr)oxides (Komarek et al., 2013) (e.g. ferrihydrite) with high surface area and sorption capacity. Due to their variable surface charge and large number of reactive terminal hydroxyl groups, they can adsorb both anions and cations. The sorption is pH-dependent with stronger sorption of anions at low pH (higher net positive surface charge) and stronger sorption of cations at high pH. At intermediate pH values both cations and anions may be strongly sorbed. Further, trace elements can be co-precipitated with newly-formed iron (hydr)oxides (Komarek et al., 2013). Critical factors that affect the immobilization capacity of oxidized ZVI include pH and redox conditions, the volume of infiltrating water and microbial activity (Kumpiene et al., 2007), as well as the rate of crystallization of the formed iron (hydr)oxides (Cundy et al., 2008).

Heavy metals, such as copper(II), form strong complexes with organic matter and adsorb strongly to metal (hydr)oxides as inner-sphere surface complexes (Karlsson et al., 2006; Peacock and Sherman, 2004; Scheinost et al., 2001). Both complex formation and adsorption are strongly pH-dependent and increase with increasing pH. Still, the soil solution copper concentration often increases at pH >6-7 due to the dissolution of solid organic matter (SOM) and subsequent release of organically bound copper(II) (Dijkstra et al., 2004). The effect of ZVI addition has previously been investigated for some copper-contaminated soils. Hartley et al. (2004) reported no effect of ZVI addition on readily extractable copper. By contrast, Bes and Mench (2008) evidenced decreased copper concentration in the soil solution, and Kumpiene et al. (2006) observed decreased exchangeable copper concentrations following ZVI addition. Furthermore, Kumpiene et al. (2011) investigated the effect of a mixture of ZVI and compost on copper speciation in a contaminated soil two years after treatment through a combination of extended X-ray absorption fine structure (EXAFS) spectroscopy and sequential extraction. It was revealed that copper was mainly associated with organic matter in the untreated soil (pH 6.2), whereas a large part was associated with iron (hydr)oxides in the soil treated with ZVI and compost (pH 7.0) (Kumpiene et al., 2011). The increased content of iron (hydr)oxides as well as a higher pH increased the copper binding to iron (hydr)oxides in the treated soil.

Arsenate is strongly bound as inner-sphere surface complexes to iron and aluminum (hydr)oxides in soils (Hopp et al., 2008; Violante and Pigna, 2002). Earlier investigations of ZVI-stabilized As-contaminated soil (Komarek et al., 2013; Mench et al., 2006) indicated that As was present as arsenate despite the fact that ZVI is a rather powerful reducing agent (Cundy et al., 2008). Other oxyanions in the soil solution, such as phosphate, compete with arsenate for sorption sites (Manning and Goldberg, 1996; Violante and Pigna, 2002). By contrast, cations increase arsenate sorption by affecting the electrostatic interactions at the

solid/solution interface (Antelo et al., 2015). In soils with a high content of organic matter, humic substances occupy sorption sites as they react with iron and aluminum (hydr)oxides (Gustafsson, 2006), thus decreasing the efficiency of the ZVI amendments.

Although ZVI can immobilize several contaminants including arsenic, copper and chromium in a short-term perspective (months to a few years) (Cundy et al., 2008; Kumpiene et al., 2006), questions about the long-term performance (several years) remain to be answered before this technique can be recommended with confidence by regulators. In particular, detailed knowledge is needed about the immobilizing mechanisms involved and how they might change with time. Reviews on chemical stabilization of soils highlight the need for long-term field studies (Cundy et al., 2008; Komarek et al., 2013; Kumpiene et al., 2008). In this work we used a combination of batch experiments, geochemical modeling and EXAFS spectroscopy to investigate the long-term performance of ZVI in soils contaminated with copper or arsenic. A multisurface geochemical model can, if confirmed to work well for contaminated soils, be used to optimize ZVI application rates and chemical conditions for contaminant immobilization. EXAFS spectroscopy provides information of bonding mechanisms on a molecular scale, which can verify the speciation results obtained with the geochemical model. It was therefore important to use a geochemical model that could account for variable chemical conditions and be verified by EXAFS measurements. For mineral surfaces this can only be done by a SCM. Here ZVI-treated soils from two field experiments, one copper-contaminated soil stabilized 6 years before sampling and one arsenic-contaminated soil stabilized 15 years before sampling, were evaluated. To our knowledge this is the first time a surface complexation model (SCM) for iron (hydr)oxides was used to predict the efficiency of metal(oid) stabilization in soils amended with ZVI. In this study we aim to: (1) quantify the long-term effect of ZVI amendments on dissolved arsenic and copper in a wide pH range (4-8), (2) identify the mechanism(s) responsible for immobilization and

(3) set up a geochemical model able to predict dissolved copper and arsenic under different scenarios.

2. Materials and Methods

2.1. Soil Sampling and Characterization

Samples from a copper-contaminated soil were collected in March 2012 at a former wood preservation site in Saint Médard d'Eyrans, France. The soil copper contamination depended on sub-sites, with up to 2600 mg Cu kg^{-1}, due to wood treatment with preservatives containing copper salts such as copper(II) sulfate (Bes and Mench, 2008). Field plots with different stabilizing amendments were established at the site in 2006, and different aspects of stabilization and phytoremediation have been studied since then (Bes and Mench, 2008; Kumpiene et al., 2011; Mench and Bes, 2009). The soil is sandy, contains about 6% clay and has been classified as a Fluvisol (Mench and Bes, 2009). Patches of *Agrostis capillaris* L. were established on CuUNT soil, whereas patches of *A. capillaris* and *Rumex acetosella* L. colonized the CuZVI soil (Bes et al., 2010). Samples of untreated soil (CuUNT) and soil stabilized with 2 wt-% ZVI (CuZVI) were collected from the top soil (0-20 cm) of the P7 subsite (Bes and Mench, 2008). The arsenic-contaminated soil originates from a former agricultural field close to a derelict arsenic(III) refinery in Reppel, Belgium. The soil is sandy, contained about 5% clay, was classified as a Podzol (Mench et al., 2006) and had been contaminated with up to 600 mg As kg^{-1}. The topsoil (0-14 cm) was stabilized with ZVI amendments, placed in large outdoor lysimeters in 1997 in plots that were cultivated, first with maize and vegetables (Mench et al., 2006) and later with an arsenic hyperaccumulator (*Pteris vittata* L.) (Mench et al., 2014). Samples of untreated soil (AsUNT) and of soil stabilized with 1 wt-% ZVI (AsZVI) were collected from the lysimeters in March 2012. The ZVI used for stabilization contained 97% metallic iron and small amounts of impurities (Mn

and Cr <1%, Ni, Al and Cu ≤ 0.1%) (Bes and Mench, 2008; Mench et al., 2006). After sampling, the soils were air-dried, homogenized and sieved.

Arsenic, copper and iron concentrations in soil samples were determined with ICP-SFMS (EPA 200.8) after digestion with HNO_3 + H_2O_2 (As and Cu) or melting with $LiBO_2$ and subsequent digestion with HNO_3 (Fe). Metal and major cations participating in equilibrium reactions, the "geochemically active concentrations" of these ions, were extracted with 0.1 M HNO_3 (16 h) (Gustafsson and Berggren Kleja, 2005). Poorly crystalline iron and aluminum (hydr)oxides as well as co-adsorbed arsenic were extracted with oxalate/oxalic acid buffer at pH 3.0 (Reeuwijk, 1995). The elemental composition in the extracts was determined with ICP-SFMS. Total organic carbon in air-dried soil samples was determined after combustion using a LECO CNS-2000 analyzer (LECO, St. Joseph, MI).

2.2. Batch experiments

Three gram of air-dried soil, sieved to <3.15 mm, was added to 30 mL solution in polypropylene centrifuge tubes. The ionic strength and pH were adjusted by adding appropriate amounts of $NaNO_3$, HNO_3 and/or NaOH to cover a pH range from 4 to 8 and to give a final NO_3^- concentration of 0.01 mol L^{-1}. All samples were prepared in duplicate. The suspensions were shaken on an end-over-end shaker for 5 days at 21^oC. After equilibration, the samples were centrifuged for 20 minutes at 2600*g*. The pH of the supernatant was measured, and the remaining sample was filtered through 0.2 µm single-use filters (Supor® Acrodisc®). Phosphate was measured colorimetrically using a Seal Analytical AA3 Autoanalyzer. Dissolved organic carbon (DOC) was determined using a Shimadzu TOC 5000 analyzer. Metal and arsenic were analyzed with ICP-SFMS after acidification to a concentration of 1% concentrated HNO_3.

2.3. Geochemical modeling

Dissolved copper and arsenic in untreated and ZVI-treated soils were simulated with a multisurface geochemical model designed in the Visual MINTEQ 3.1 software (Gustafsson, 2013). The model included speciation in the dissolved phase, sorption/desorption to iron and aluminum (hydr)oxide sorbents, binding to SOM, and precipitation/dissolution of minerals. Modeling was performed using a priori assumptions on amounts and properties of reactive surfaces, total concentrations of "geochemically active" concentrations etc., based on chemical analyses. No calibration of the model was performed for the investigated samples.

Sorption to iron and aluminum (hydr)oxide sorbents was modeled with a SCM, the Three Plane CD-MUSIC model (Hiemstra and van Riemsdijk, 1996; Hiemstra and van Riemsdijk, 2006) using the surface charging parameters of Tiberg et al., (2013) i.e. both iron and aluminum (hydr)oxide were assumed to behave as ferrihydrite. The surface complexation reactions and constants can be found in the Supplementary Material (SM), Table S1. Crystalline (hydr)oxides and clay minerals were assumed to be of minor importance for sorption and were therefore not considered. The CD-MUSIC model was used, rather than the most widely used SCM for ferrihydrite, the generalized two layer model (GTLM) (Dzombak and Morel, 1990), because it is more advanced in the description of the surface sites and electrostatics but easy to use once it is parameterized. The CD-MUSIC model is a 1-pK three-plane model. Unlike other SCMs it relates the distribution of charge in the Stern layer to the structure of surface complexes. In agreement with the results and modeling of Gustafsson and Bhattacharya (2007) and Tiberg et al. (2013), the sorption of copper(II) and arsenate was dominated by bidentate coordination to the ferrihydrite surface. A doubly protonated arsenate-ferrihydrite complex is also included but only important at low pH. Complexation to organic matter was modeled with the Stockholm Humic Model (SHM) using the acid-base parameters of Gustafsson & van Schaik (2003). These models are both present in Visual MINTEQ 3.1.

Ferrihydrite and $Al(OH)_3(s)$ were included as solid phases, i.e. they were formed if their saturation indices were ≥1 and then controlled the activity of Fe^{3+} and Al^{3+} in solutions. The solubility constants used were $*K_s = 10^{2.93}$ for ferrihydrite (Liu and Millero, 1999) and $10^{8.54}$ for $Al(OH)_3(s)$ (Gustafsson et al., 1998), at 21°C.

Model entries:

- Geochemically active concentrations of Cu, Mg, Ca, K as extracted by 0.1 mol L^{-1} HNO_3 and As as extracted by oxalate/oxalic acid (SM Table S1).
- Fe and Al as extracted by oxalate/oxalic acid (SM Table S1).
- Concentration of Na^+ and NO_3^-, as added (0.01 mol L^{-1}).
- DOC and phosphate in equilibrium solutions, as determined for each pH value (SM Table S2).
- The concentration of inorganic sorbents determined using the following procedure: oxalate-extractable Fe and Al were entered into the model. For each pH value, the model calculated the equilibrium partitioning of Fe and Al in solution, bound to organic matter and precipitated as ferrihydrite and $Al(OH)_3(s)$. The sum of ferrihydrite and $Al(OH)_3(s)$ concentrations constituted the total sorbent concentration in the CD-MUSIC model (SM Table S2).
- The concentration of 'active' SOM, i.e. active with respect to proton and metal binding, was assumed to constitute 50% of the total organic matter, which in turn consited of 50% C by weight. This is reasonable based on previous findings for mineral soils (Gustafsson and Van Schaik, 2003). The active SOM was assumed to consist of 50% humic acid (HA) and 50% fulvic acid (FA).
- The ratio of 'active' dissolved organic matter (DOM) to DOC was set to 2, and DOM was assumed to consist of 100% FA.

2.4. X-ray absorption spectroscopy (XAS)

Dried soil samples were ground in a ball mill before analysis to homogenize the samples and reduce particle size. They were then packed in aluminum frames and sealed with tape. To aid the interpretation of soil XAS spectra standard spectra for copper and arsenate bound to ferrihydrite, amorphous aluminum hydroxide and fulvic acid were used (see SM Table S5, for details on preparation).

XAS spectra of copper-contaminated soil samples were collected at the copper K edge at 8,979 eV at the wiggler beam line I811, MAX-Lab, Lund, Sweden. Standard spectra for arsenate adsorbed to ferrihydrite and amorphous aluminum hydroxide were collected at the same beamline at the arsenic K edge at 11,867 eV. XAS measurements of arsenic-contaminated soil samples and copper bound to ferrihydrite, amorphous aluminum hydroxide and fulvic acid were performed at the arsenic and copper K-edges at the wiggler beam line 4-1, Stanford Synchrotron Radiation Lightsource (SSRL), Stanford, USA. More details can be found in the Supplementary Material.

All XAS spectra were treated in the Athena software (version 0.9.20) (Ravel and Newville, 2005). The background was removed using the AUTOBAK algorithm incorporated in Athena, with a *k*-weight of 2 or 3 and with the Rbkg parameter set to 1 for the copper spectra and to 0.85 for the arsenic spectra. A model of the first shell was used to improve the background of arsenic spectra as described by Kelly et al. (2008). Wavelet transform (WT) analysis of the EXAFS spectra (Funke et al., 2005) was performed to differentiate between light (e.g. C, O) and heavy (e.g. Fe) elements (back-scatterers) at 2.5-4.5 Å from the measured element. This qualitative analysis of backscattering contributions from higher shell atoms was performed with the Morlet WT incorporated in the Igor Pro script (Chukalina, 2010) with the parameter combination κ = 7 (Cu) or 6 (As), σ = 1 and with a range of $R + \Delta R$ from 2 to 4 Å

(corresponding to interatomic distances of about 2.5 to 4.5 Å). The *k*-ranges were the same as in the EXAFS fitting procedure.

Final data treatment of the EXAFS spectra was performed with the Artemis software (version 0.0.012) (Ravel and Newville, 2005). Theoretical scattering paths were calculated with FEFF6 (Zabinsky et al., 1995). During the fitting procedure the amplitude reduction factor (S_0^2) was set based on fitting of this parameter for the first coordination shell. The spectra of the standards were fit first and the resulting interatomic distances, as well as distances from literature, were then used in the modeling of soil samples. Several combinations of scattering paths were tested in the fitting procedure before deciding what paths to use; these included Cu/As–O, Cu···C, Cu/As···Fe and Cu/As···Al distances and multiple scattering (MS) paths. The coordination numbers (CN) were fixed. The path lengths (R) and Debye-Waller factors (σ^2) were fitted with the exception of σ^2 of the MS within the arsenate tetrahedron, which was set to the same value as for the As–O path. Values of CN were chosen to give reasonable values of σ^2. Cu···C paths were calculated using FEFF6 (Zabinsky et al., 1995) based on a 5-member chelate ring structure. The Cu···Fe paths used in the final fits were based on the mineral structure of cornetite (Eby and Hawthorne, 1989), with partial Fe-for-Cu substitution. Arsenic(V) scattering paths were based on the structures of scorodite (Xu et al., 2007) and mansfieldite (Harrison, 2000). The fitting procedure was performed on the Fourier transform real part between 1 and 4 Å using a Hanning window (dk value = 1) and optimizing over k-weights of 1, 2 and 3. Refined models were evaluated by means of goodness-of-fit (as evidenced by the R factor in Artemis) and qualitative comparison of WT plots of the model spectra with WT plots of the EXAFS spectra. WT of the model spectra were made with the same WT-parameters and k-ranges as for measured spectra.

3. Results and discussion

3.1. Soil properties

The pH was about 6 in the copper and 8 in the arsenic-contaminated soil (Table 1). This is in agreement with the markedly higher calcium and magnesium concentrations (5-10 times) in the arsenic contaminated soil compared to the copper-contaminated soil (SM, Table S3 and S4). Both soils were rather low in organic matter, having an organic carbon concentration of ca 1%. Notably, the concentration was lower in the ZVI-treated samples at both sites (Table 1), which may influence the dissolved copper concentration. The pseudo-total concentration of iron (Fe_{tot}) was 1.9 wt% higher in CuZVI compared to CuUNT and 1.0 wt% higher in AsZVI than in AsUNT (Table 1), which is in perfect agreement with the added amounts. The oxalate-extractable aluminum concentrations were of the same magnitude as oxalate-extractable iron in the untreated soils and in the AsZVI soil. The oxalate-extractable fraction of Fe_{tot} was 57% in CuZVI, compared to 12% in CuUNT, i.e. 77% of the added ZVI remained oxalate-extractable 6 years after application in this soil. As oxalate/oxalic acid primarily extracts poorly crystalline iron (hydr)oxides (Parfitt and Childs, 1988) and this means that a majority of added ZVI was present in poorly crystalline forms such as ferrihydrite. In AsZVI, the fraction of oxalate-extractable iron was lower, corresponding to 30% of added ZVI. This indicates that some of the added ZVI had been converted to more crystalline forms such as goethite in this soil (Parfitt and Childs, 1988). A likely explanation for the smaller fraction of poorly crystalline iron (hydr)oxides in this soil compared to CuZVI is the longer time since application (15 years). The pseudo-total soil arsenic (As_{tot}) was the same in AsUNT and AsZVI but the pseudo-total soil copper (Cu_{tot}) was considerably higher in CuZVI than in CuUNT (Table 1). Although the ZVI grit contains copper as an impurity this cannot be the main explanation as 0.1% copper in the ZVI grit (Bes and Mench, 2008) would only give an extra 0.3 mmol kg^{-1} of copper. Possible reasons include (i) inhomogeneous distribution of copper in the soil, and (ii) a larger copper leaching in the untreated soil and differences in

copper plant uptake. The geochemically active concentrations of copper in CuUNT and CuZVI as well as arsenic in AsUNT and AsZVI (Table 1) were close to the total concentrations, i.e. most of the copper and arsenic should be able to react readily with the soil solution.

Table 1

Chemical properties and main contaminants of the investigated soil samples

Sample	Org. C	pH[a]	Fe_{ox}[b]	Al_{ox}[b]	Fe_{tot}[c]	Cu_{tot}[c]	Cu_{act}[e]	As_{tot}[c]	As_{act}[e]
	%		mmol kg^{-1} dw		mmol kg^{-1} dw				
CuUNT	1.14	6.00	19	25	154	6.1	5.6		
CuZVI	0.59	6.47	283	18	496	11.0	10.2		
AsUNT	1.24	7.79	25	40	109			1.4	1.2
AsZVI	0.98	7.95	79	39	289			1.4	1.4

[a] pH measured in the batch experiment (0.01 M $NaNO_3$, 5 d equilibration).

[b] Subscripts ox denote oxalate extracts.

[c] Pseudo-total concentration (Method section).

[e] "Geochemically active" concentration, as obtained from extraction with 0.1 M HNO_3 (Cu) or oxalate/oxalic acid buffer (As).

3.2. Dissolved concentrations of copper and arsenic

As expected, dissolved copper (copper(II) ions and dissolved complexes) was highly pH-dependent in both untreated and ZVI-treated soil samples, with minimum dissolved concentrations at about pH 6-7 (Fig 1a, SM Table S3). Dissolved copper was lower in CuZVI compared to CuUNT at pH >6 and 70% lower at ambient soil pH. The higher concentration of soluble copper at low pH in the ZVI-treated soil was explained by a combination of higher copper concentration and lower SOM concentration in this sample compared to CuUNT (Table 1). A higher concentration of SOM (8-14%) combined with a lower ZVI addition (1

wt-%) may be the reasons why Hartley et al. (2004) did not obtain a stabilizing effect on copper by ZVI in spite of a pH >6 in their soils. In other studies where ZVI addition did lower the copper concentration in the soil solution (Bes and Mench, 2008) or exchangeable copper (Kumpiene et al., 2006) the SOM content was lower.

The dissolved arsenic concentration was lower in AsZVI compared to AsUNT in the whole pH range, but the immobilizing effect increased with decreasing pH (Fig 1b). At the original soil pH (about 8), dissolved arsenic was reduced by 50% in AsZVI compared to AsUNT, whereas at pH 5 dissolved arsenic decreased by 95% as a result of ZVI stabilization. In an earlier study at the same site, performed six years after ZVI treatment, the arsenic concentrations were about 85% lower in the leachate from the ZVI-treated soil at pH ~7 (Mench et al., 2006) which agrees with our study that predicts about 70-80% less dissolved arsenic at pH 7 (Fig 1b). In other words an additional period of 9 years did not significantly reduce the stabilizing effect of ZVI on arsenic.

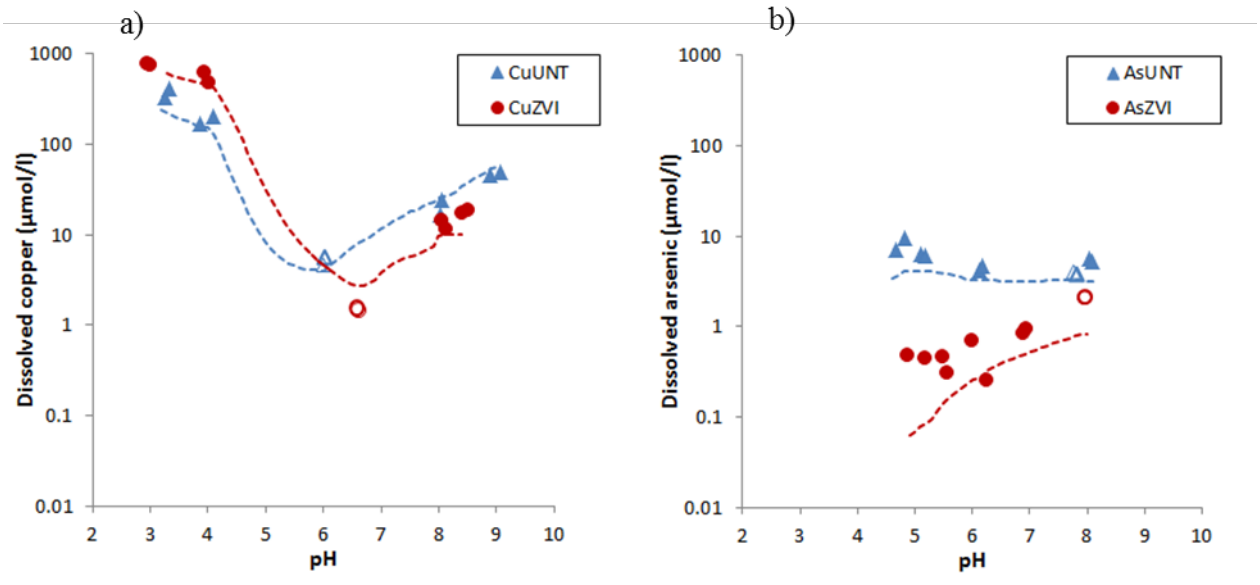

Fig 1. Dissolved copper and arsenic as a function of pH; results from batch experiments and geochemical modeling. (a) Cu; CuUNT (triangles), CuZVI (circles) and models (dashed

lines). (b) As; AsUNT (triangles), AsZVI (circles) and models (dashed lines). Open symbols are experimental points at soil pH.

As mentioned above, generic parameters and "standard" assumptions were used in the modeling. Bearing this in mind, model-predicted concentrations of dissolved copper agreed well with the measured concentrations, both in the untreated and in the ZVI-treated soils (Fig 1a). This indicates that the model is able to describe the major retention mechanisms and their pH dependence, i.e. dissolved copper was controlled by surface complexation reactions to SOM and iron/aluminum (hydr)oxides, and by complexation to DOM in solution (Fig 2). Furthermore, the good agreement between experimental data and model simulations provides indirect support for the assumption (based on oxalate extraction data) that the major fraction of the ZVI had been transformed into ferrihydrite..

The modeled concentrations of dissolved arsenate followed the trend of the experimental results well, although they were generally somewhat underestimated, particularly in the ZVI-treated soil. One possible explanation is that, for this soil, oxalate does not provide a precise estimate of the concentration of poorly crystalline metal (hydr)oxides corresponding to the amount of ferrihydrite in the model. As shown below, reducing the fraction of ferrihydrite from 30 to 15% of the total iron content improved the fit (Fig. 6). Factors that might have contributed to the discrepancy between modeled and measured results are ageing effects such as aggregation and ordering of the ferrihydrite (Dale et al., 2015; Vu et al., 2013), not captured by the oxalate extraction. Another contributing factor could be blocking of reactive sites by humic substances (Gustafsson, 2006), which was not considered in the modeling.

3.3. Immobilization mechanisms

The simulations in Visual MINTEQ predicted that the bound copper was primarily associated with SOM within the whole pH range in CuUNT (Fig 2a), whereas there was a

shift towards sorption to the metal (hydr)oxides in CuZVI, especially at high pH (Fig 2b). At soil pH, 10% of copper was bound to iron and aluminum (hydr)oxides, compared to 70% in CuZVI. Kumpiene et al. (2011) investigated soil from the same field experiment and sub-site, but stabilized with ZVI and compost, two years after stabilization. In their study, the soil pH was 6.2 in the untreated soil compared to 7.0 in the stabilized soil, and sequential extractions indicated that the fraction of copper associated with poorly crystalline iron (hydr)oxides increased from 20% to 50% after stabilization, which is in line with our results. The simulations of arsenic partitioning predict that arsenic was only bound to iron and aluminum (hydr)oxides both in AsUNT and AsZVI.

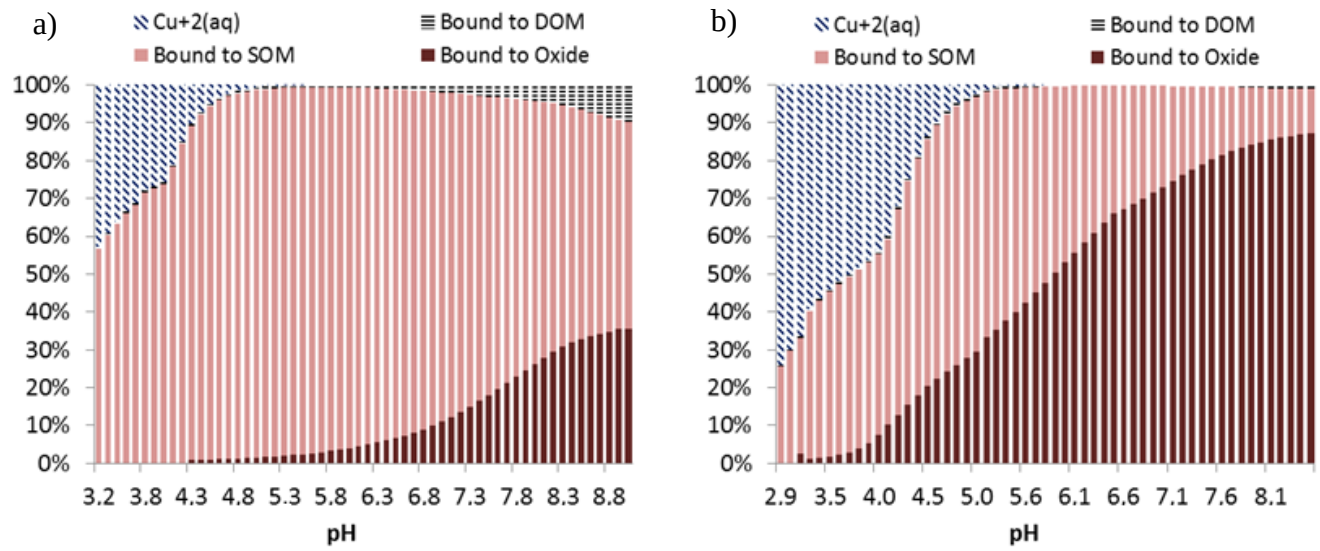

Fig 2. Modeled copper partitioning in the batch experiments. (a) CuUNT, and (b) CuZVI.

Direct information on the major binding mechanisms was available from the XAS measurements. The EXAFS spectra of soil and standard samples were first visually compared to get an indication of the arsenic and copper coordination environments in the samples. Detailed information on the coordination environment was then obtained by models of the

EXAFS spectra (see Method section). The EXAFS modeling results are summarized in the text and further discussed in the Supplementary material (SM) where all fitting parameters are presented (SM, Table S7).

Visual comparison between the EXAFS spectra of copper contaminated soil and copper standards (Fig 3a) revealed similarities between the CuUNT and copper complexed by fulvic acid on the one hand and between CuZVI and copper adsorbed to ferrihydrite on the other. The shaded area at k = 7-8 in Fig 3a highlights one example where the EXAFS spectra for CuZVI and Cu-ferrihydrite are considerably flatter than the spectra for CuUNT and Cu-fulvic acid.

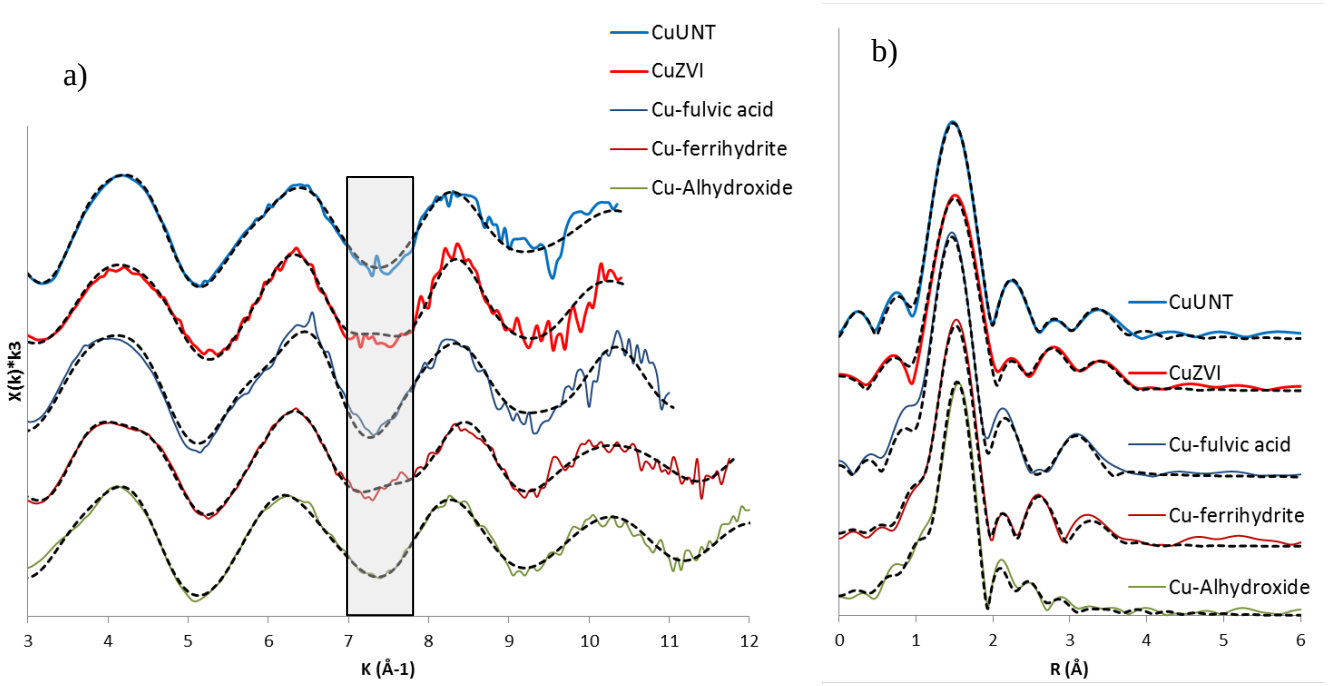

Fig 3. a) Stacked k^3-weighted K-edge EXAFS spectra for copper, and (b) Fourier transforms (FT magnitudes) of the k^3-weighted EXAFS spectra. Solid lines are raw data and dashed lines are model fits. The shaded region highlights an area where spectra for CuZVI and Cu-ferrihydrite samples are flatter than the other spectra.

There was no indication of heavy elements in the WT analysis of the Cu-fulvic acid and CuUNT spectra (SM, Fig S1, S2). In WT plots of the CuZVI and the Cu-ferrihydrite spectra heavy elements were indicated at a distance of about 3-4 Å from copper (SM, Fig S2 and Tiberg et al. (2013)). In the Cu-ferrihydrite sample this signal was earlier concluded to be iron (Tiberg et al., 2013). Thus, the WT analysis was in agreement with the EXAFS model fit, i.e. it showed that a shift from organic complexation in CuUNT to binding by iron(hydr)oxides in CuZVI had occurred.

According to EXAFS spectroscopy, copper was bound to four oxygens at about 1.95 Å in the first shell (SM, Table S7), consistent with a Jahn-Teller-distorted octahedron (Persson et al., 2002). A contribution from nitrogen functional groups could not be ruled out as backscattering from oxygen cannot be differentiated from nitrogen by EXAFS. Both the models of Cu-fulvic acid and CuUNT included back-scattering from four carbon atoms at about 2.8 Å and an MS path, Cu···C–O, at ~3 Å (SM, Table S7). These distances imply that copper was bound in a copper(II)-chelate ring structure (Karlsson et al., 2006; Strawn and Baker, 2009). Chelate rings are common in different kinds of organic molecules, for example in humic substances and biomolecules, as they stabilize copper(II) (Karlsson et al., 2006).

The Cu-ferrihydrite EXAFS spectrum was evaluated previously (Tiberg et al., 2013); copper was found to bind to ferrihydrite mainly as an inner-sphere edge-sharing complex with a Cu···Fe distance of 3.02 Å. The model of the Cu-Al-hydroxide spectrum includes a Cu···Al distance (2.97 Å) consistent with copper forming a similar complex on aluminum hydroxide (Cheah et al., 1998). In CuZVI, back-scattering from higher shells was dominated by iron at 3.09 Å implying that copper was primarily bound as inner-sphere bidentate complexes with iron (hydr)oxide (Peacock and Sherman, 2004; Scheinost et al., 2001). This was also the complex used for sorption to ferrihydrite in the SCM. Elements such as iron and copper, which are close to each other in the periodic table, cannot be distinguished in EXAFS

measurements, but a significant contribution from copper(II) dimers was unlikely as the Cu···Cu distance of a copper dimer would be about 2.9 Å (Peacock and Sherman, 2004), a distance that did not improve fits for either CuUNT or CuZVI. Thus, the EXAFS interpretations confirmed the geochemical modeling results, i.e. copper was bound almost exclusively to organic matter in the CuUNT soil (at pH 6.0) but primarily by inner-sphere complexes with iron (hydr)oxides in the CuZVI soil (at pH 6.5).

The position of the peak of the arsenic edge at about 11,874.5 eV in both soil samples (not shown) confirmed the assumption that arsenic is present as arsenate. The EXAFS spectra of the AsUNT and AsZVI samples were similar in shape indicating that arsenic was bound in a similar manner in both samples (Fig 4a, SM Fig S7).

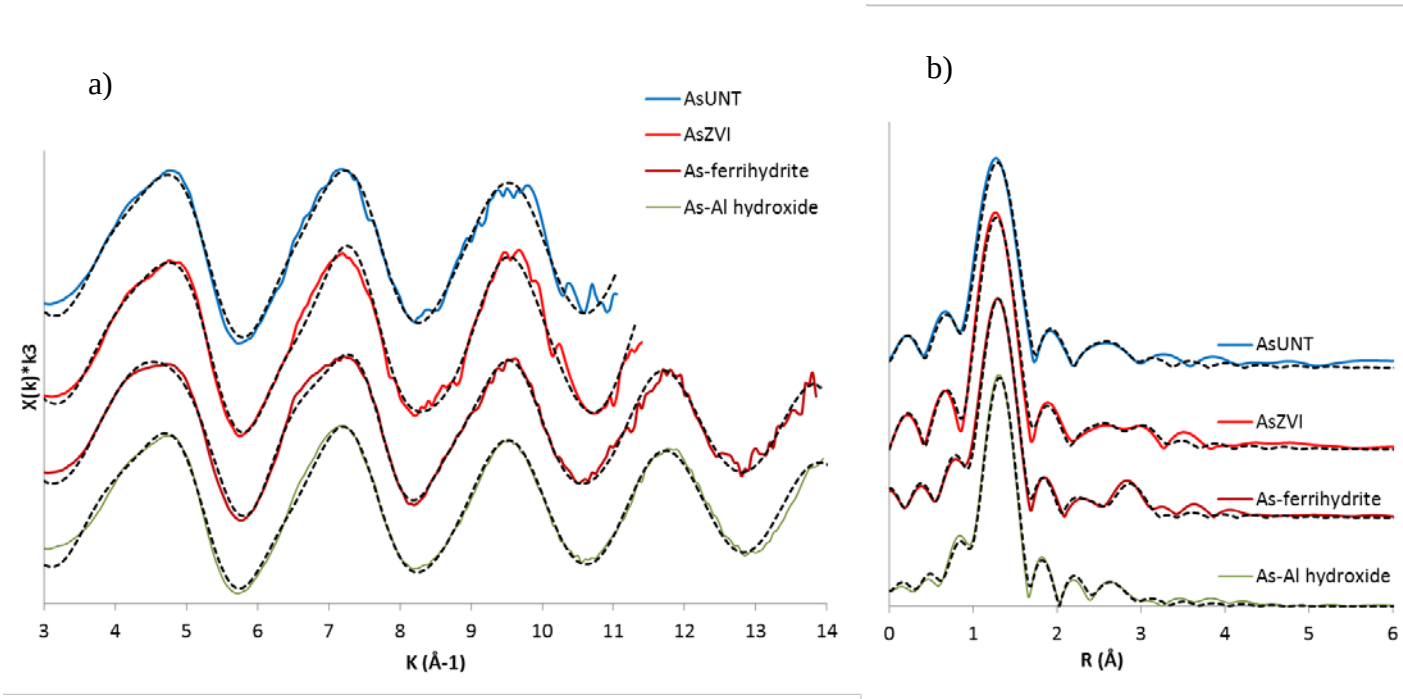

Fig 4. a) Stacked k^3-weighted K-edge EXAFS spectra for arsenic, and (b) Fourier transforms (FT magnitudes) of the k^3-weighted EXAFS spectra. Solid lines are raw data and dashed lines are model fits.

Back-scattering from elements heavier than oxygen was indicated between about 2.8 and 3.7 Å from arsenic in all WT analysis of arsenic samples (WT analysis, SM Fig S4 and S5). In all model spectra for the arsenic samples (Fig 4, SM Table S7) arsenic was surrounded by four oxygens at about 1.70 Å, consistent with an arsenate tetrahedron (Mähler and Persson, 2013). The model of the As-ferrihydrite spectra included an As···Fe distance at ~3.3 Å which indicates the formation of inner-sphere bidentate corner-sharing complexes on the ferrihydrite surface (Manceau, 1995; Sherman and Randall, 2003). The As-Al-hydroxide spectrum was modelled with two Al at ~3.2 Å, which suggests inner-sphere corner-sharing complexation of arsenic to amorphous aluminum hydroxide as well (Arai et al., 2005; Xiao et al., 2015). Bidentate coordination of arsenate to both the ferrihydrite and aluminum (hydr)oxide surfaces supports the approach to use bidentate complexes for arsenate sorption to iron- and aluiminum (hydr)oxides in the surface complexation model.

The EXAFS spectra of arsenic-contaminated soils were best fit with As···Al and As···Fe distances close to those of the standard spectra. The AsUNT spectrum was dominated by back-scattering from aluminum (As···Al 3.19 Å) whereas the AsZVI spectrum had contributions from both aluminum (As···Al 3.19 Å) and iron (As···Fe 3.39 Å) (Fig 4, parameters in SM, Table S7); both were necessary to include for a satisfactory fit. An As···Fe distance of about 3.3 Å is also consistent with the As···Fe coordination on goethite (Loring et al., 2009). Consequently the EXAFS interpretation implies that arsenate was primarily complexed to aluminum hydroxides in the AsUNT and that surface complexation to both aluminum and that iron (hydr)oxide was important in AsZVI. It is well known that arsenate adsorbs strongly to both aluminum and iron (hydr)oxides in soil (Hopp et al., 2008; Manning, 2005) and both are stable at the pH (almost 8) of the samples. Oxalate-extractable aluminum and iron (Table 1) indicated about 1/3 iron and 2/3 aluminum (hydr)oxides in AsUNT while

the relation was the opposite, 2/3 iron and 1/3 aluminum (hydr)oxides in AsZVI which agrees well with the EXAFS interpretations.

3.4. Scenario simulations

The multisurface geochemical model, verified by the batch experiments and the EXAFS measurements, was used to examine some key soil factors affecting the potential success of ZVI stabilization. For copper, organic carbon, ZVI concentrations and pH are all critical parameters. Simulations were performed on two hypothetical soils having the same soil properties as CuUNT, except that the available copper concentration was 1 mmol L^{-1} and the organic matter content 0.5 or 2% organic carbon. Calculations were made for two different ZVI applications (1% and 2%). All input data is given in Table S6 (Supplementary material). The results illustrated that immobilization of copper with ZVI is dependent not only on the pH but also on the organic matter content. ZVI had a larger effect on dissolved copper in the soil with 0.5% organic C (Fig. 5a) than in the soil with 2% organic C although the overall dissolution of copper was lower in the soil with more organic matter, especially at low pH. This illustrates that stabilization of copper with ZVI would be most effective in soils with a pH above 6 that are relatively low in organic matter.

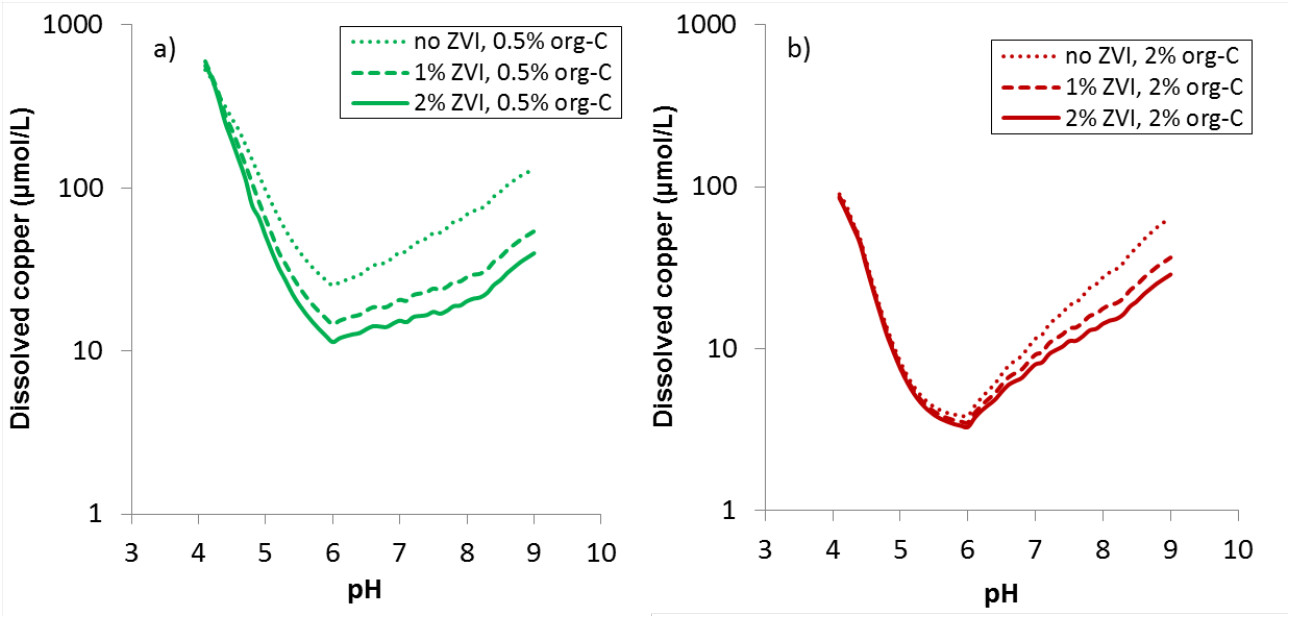

Fig 5. Simulations of how soil organic matter content and ZVI addition affect dissolved copper concentrations. Dashed lines simulate 1% of ZVI added and solid lines simulate 2% of ZVI added to soils with different contents of organic material, a) 0.5% organic C and b) 2% organic C.

As shown above, the geochemical model underestimated dissolved arsenate (Fig. 1). Experimental data were simulated more accurately by decreasing the amount of "active" iron/aluminum (hydr)oxide, as compared to what was estimated by the oxalate extraction. Much improved fits were obtained by decreasing the number of sorption sites by 30% in AsUNT and by 50% in AsZVI (Fig 6a). This might reflect either a tendency for oxalate to overestimate the amount of arsenate sorption sites in this soil or a need to compensate for the ageing of ferrihydrite and/or blocking of sorption sites by humic substances.

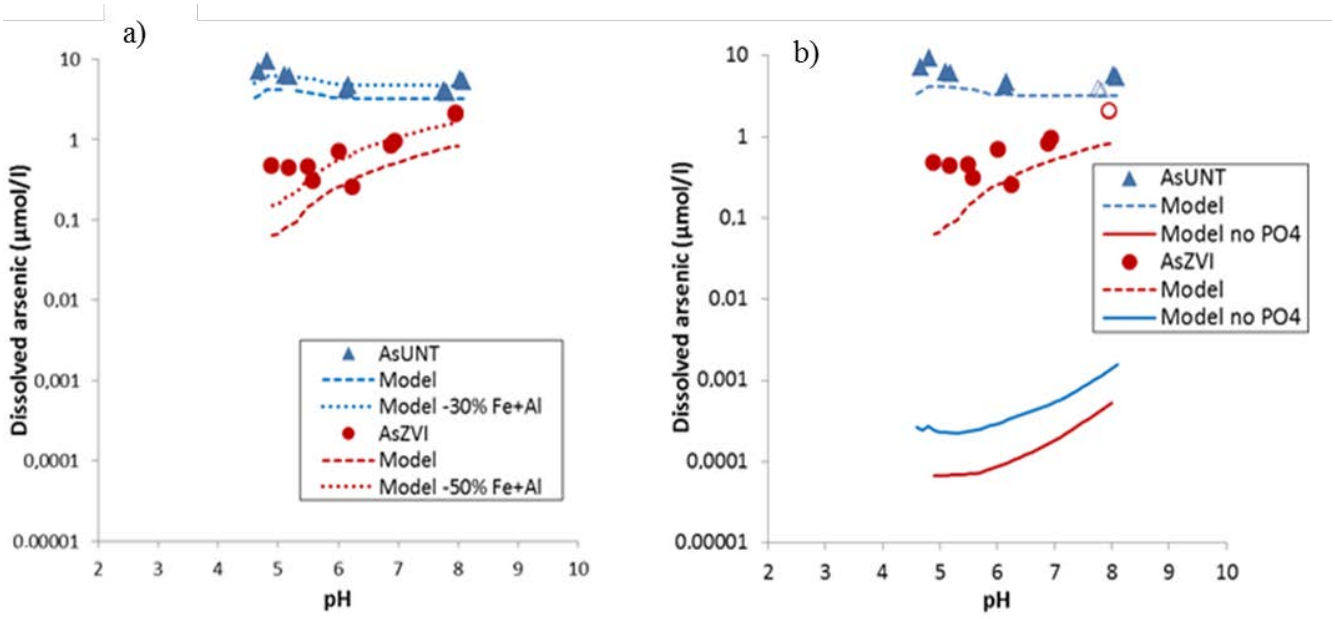

Fig 6. Simulation of dissolved arsenate at different modeling scenarios. Measured concentrations: AsUNT (triangles) and AsZVI (circles). The "original" model is shown for comparison (dashed lines). a) Model with 30% (AsUNT) and 50% (AsZVI) less (hydr)oxide (dotted lines). b) Model with no competing phosphate ions (solid lines).

Figure 6b illustrates the effect of the competition for sorption sites between arsenate and phosphate. Arsenate and phosphate has a similarly high affinity for sorption to ferrihydrite and aluminum (hydr)oxides and compete for the same sorption sites (Gustafsson and Bhattacharya, 2007; Violante and Pigna, 2002). There were significant amounts of phosphate in the arsenic-contaminated soil; the phosphate concentration in the supernatant of the batch experiments was about 10 times higher than the arsenate concentration. If phosphate was ignored in the modeling, arsenate sorption was more than 1,000 times overestimated (Fig 6b). Thus, in situations in which soil fertility needs to be improved as part of a GRO option involving ZVI amendment, care should be taken when optimizing phosphate fertilizer application rates. In this respect, appropriately calibrated geochemical models, such as Visual MINTEQ, can be useful tools.

4. Conclusions

The results of this study imply that:

- The effects of ZVI amendment are long-lasting. Stabilization was in effect 6 and 15 years after ZVI incorporation under field conditions into both investigated soils.
- The dissolution of copper and arsenic in ZVI-treated soils can be described by surface complexation reactions also in long-term aged soils.
- It is important to consider the pH value of the soil to be treated with ZVI. For copper, stabilization with ZVI is usually not applicable if the pH is lower than about 6, which is consistent with known sorption behavior of copper(II) to iron (hydr)oxides. Arsenate is less pH-sensitive, but immobilization is improved at low pH values.
- As copper form strong complexes both with iron (hydr)oxides and organic matter stabilization with ZVI is more effective when content of organic matter in the soil is low.
- Competition with phosphate has to be included when evaluating arsenate sorption in soils, because of the strong competition between these ions. If phosphate is ignored, sorption of arsenate might be greatly overestimated.
- Geochemical models accounting for surface complexation processes on iron/aluminum (hydr)oxides and SOM are powerful tools that can be used to optimize ZVI treatments of contaminated soil (application rate, pH, competition for sorption sites by other ions, etc.).

Supplementary material

Geochemically active concentrations (Table S1), Ranges of pH, DOC, Fh and phosphate model entries (Table S2), results from leachability experiments (Table S3, S4), standards for XAS measurements (Table S5), Wavelet transforms of EXAFS spectra and models (Fig S1-S2, S4-S5). Superimposed EXAFS spectra of arsenic contaminated soil (Fig S3) and EXAFS model fit results (Table S6).

Acknowledgements

Part of this research was carried out at beamline I811, MAX-lab synchrotron radiation source, Lund University, Sweden. Funding for the beamline I811 project was kindly provided by The Swedish Research Council and the “Knut och Alice Wallenbergs Stiftelse”. Portions of this research were carried out at the Stanford Synchrotron Radiation Lightsource, SLAC National Accelerator Laboratory, supported by the U.S. Department of Energy, Office of Science, Office of Basic Energy Sciences under Contract No. DE-AC02-76SF00515. The SSRL Structural Molecular Biology Program is supported by the DOE Office of Biological and Environmental Research, and by the National Institutes of Health, National Institute of General Medical Sciences (including P41GM103393). The contents of this publication are solely the responsibility of the authors and do not necessarily represent the official views of NIGMS or NIH. Michel Mench is grateful for financial support to ADEME, Department of Urban Brownfields and Polluted Sites, Angers, France, and the European Commission under the Seventh Framework Programme for Research (FP7-KBBE-266124, GREENLAND).

References

Antelo, J., Arce, F., Fiol, S., 2015. Arsenate and phosphate adsorption on ferrihydrite nanoparticles. Synergetic interaction with calcium ions. Chem. Geol. 410, 53-62.

Arai, Y., Sparks, D.L., Davis, J.A., 2005. Arsenate adsorption mechanisms at the allophane - water interface. Environ. Sci. Technol. 39, 2537-2544.

Bes, C., Mench, M., 2008. Remediation of copper-contaminated topsoils from a wood treatment facility using in situ stabilisation. Environ. Pollut. 156, 1128-1138.

Bes, C., Mench, M., Aulen, M., Gaste, H., Taberly, J., 2010. Spatial variation of plant communities and shoot Cu concentrations of plant species at a timber treatment site. Plant and Soil 330, 267-280.

Bolan, N., Kunhikrishnan, A., Thangarajan, R., Kumpiene, J., Park, J., Makino, T., Kirkham, M.B., Scheckel, K., 2014. Remediation of heavy metal(loid)s contaminated soils – To mobilize or to immobilize? J. Hazard. Mater. 266, 141-166.

Cheah, S.-F., Brown, G.E., Parks, G.A., 1998. XAFS spectroscopy study of Cu(II) sorption on amorphous SiO_2 and γ-Al_2O_3: Effect of substrate and time on sorption complexes. J. Colloid Interface Sci. 208, 110-128.

Chukalina, M., 2010. Wavelet2.ipf, a procedure for calculating the Wavelet transform in IGOR Pro, http://www.esrf.eu/UsersAndScience/Experiments/CRG/BM20/Software/Wavelets/IGOR.

Cundy, A.B., Bardos, R.P., Church, A., Puschenreiter, M., Friesl-Hanl, W., Müller, I., Neu, S., Mench, M., Witters, N., Vangronsveld, J., 2013. Developing principles of sustainability and stakeholder engagement for “gentle” remediation approaches: The European context. J. Environ. Manage. 129, 283-291.

Cundy, A.B., Hopkinson, L., Whitby, R.L.D., 2008. Use of iron-based technologies in contaminated land and groundwater remediation: A review. Sci. Total Environ. 400, 42-51.

Dale, J.G., Stegemeier, J.P., Kim, C.S., 2015. Aggregation of nanoscale iron oxyhydroxides and corresponding effects on metal uptake, retention, and speciation: I. Ionic-strength and pH. Geochim. Cosmochim. Acta 148, 100-112.

Dijkstra, J.J., Meeussen, J.C.L., Comans, R.N.J., 2004. Leaching of heavy metals from contaminated soils: an experimental and modeling Study. Environ. Sci. Technol. 38, 4390-4395.

Eby, R.K., Hawthorne, F.C., 1989. Cornetite: modulated densely-packed Cu^{2+} oxysalt. Miner. and Petrol. 40, 127-136.

Funke, H., Scheinost, A.C., Chukalina, M., 2005. Wavelet analysis of extended X-ray absorption fine structure data. Phys. Rev. B 71.

Gustafsson, J.P., 2006. Arsenate adsorption to soils: Modelling the competition from humic substances. Geoderma 136, 320-330.

Gustafsson, J.P., 2013. Visual MINTEQ 3.1, http://vminteq.lwr.kth.se/.

Gustafsson, J.P., Berggren Kleja, D., 2005. Modeling salt-dependent proton binding by organic soils with the NICA-Donnan and Stockholm Humic Models. Environ. Sci. Technol. 39, 5372-5377.

Gustafsson, J.P., Bhattacharya, P., 2007. Geochemical modelling of arsenic adsorption to oxide surfaces, In: Bhattacharya, P., Mukherjee, A.B., Bundschuh, J., Zevenhoven, R., Loeppert, R.H. (Eds.), Trace metals and other contaminants in the environment. Elsevier, pp. 159-206.

Gustafsson, J.P., Van Schaik, J.W.J., 2003. Cation binding in a mor layer: batch experiments and modelling. Eur. J. Soil Sci. 54, 295-310.

Harrison, W., 2000. Synthetic mansfieldite, $AlAsO_4 \cdot 2H2O$. Acta Crystallogr. Sect. C 56, e421.

Hartley, W., Edwards, R., Lepp, N.W., 2004. Arsenic and heavy metal mobility in iron oxide-amended contaminated soils as evaluated by short- and long-term leaching tests. Environ. Pollut. 131, 495-504.

Hiemstra, T., van Riemsdijk, W.H., 1996. A surface structural approach to ion adsorption: The charge distribution (CD) model. J. Colloid Interface Sci. 179, 488-508.

Hiemstra, T., van Riemsdijk, W.H., 2006. On the relationship between charge distribution, surface hydration, and the structure of the interface of metal hydroxides. J. Colloid Interface Sci. 301, 1-18.

Hopp, L., Nico, P.S., Marcus, M.A., Peiffer, S., 2008. Arsenic and Chromium partitioning in a podzolic soil contaminated by chromated copper arsenate. Environ. Sci. Technol. 42, 6481-6486.

Karlsson, T., Persson, P., Skyllberg, U., 2006. Complexation of Copper(II) in organic soils and in dissolved organic matter − EXAFS evidence for chelate ring structures. Environ. Sci. Technol. 40, 2623-2628.

Kelly, S., Hesterberg, D., Ravel, B., 2008. Analysis of soils and minerals using X-ray absorption spectroscopy, in: Ulery, A.L., Drees, R.L. (Eds.), Methods of soil analysis. Part 5. Mineralogical methods. SSSA Book Series, SSSA, Madison, WI.

Kidd, P., Mench, M., Álvarez-López, V., Bert, V., Dimitriou, I., Friesl-Hanl, W., Herzig, R., Janssen, J.O., Kolbas, A., Müller, I., Neu, S., Renella, G., Ruttens, A., Vangronsveld, J., Puschenreiter, M., 2015. Agronomic practices for improving gentle remediation of trace element-contaminated soils. Int. J. Phytorem., 1005-1037.

Komarek, M., Vanek, A., Ettler, V., 2013. Chemical stabilization of metals and arsenic in contaminated soils using oxides - A review. Environ. Pollut. 172, 9-22.

Kumpiene, J., Castillo Montesinos, I., Lagerkvist, A., Maurice, C., 2007. Evaluation of the critical factors controlling stability of chromium, copper, arsenic and zinc in iron-treated soil. Chemosphere 67, 410-417.

Kumpiene, J., Lagerkvist, A., Maurice, C., 2008. Stabilization of As, Cr, Cu, Pb and Zn in soil using amendments – A review. Waste Manage. 28, 215-225.

Kumpiene, J., Mench, M., Bes, C.M., Fitts, J.P., 2011. Assessment of aided phytostabilization of copper-contaminated soil by X-ray absorption spectroscopy and chemical extractions. Environ. Pollut. 159, 1536-1542.

Kumpiene, J., Ore, S., Renella, G., Mench, M., Lagerkvist, A., Maurice, C., 2006. Assessment of zerovalent iron for stabilization of chromium, copper, and arsenic in soil. Environ. Pollut. 144, 62-69.

Loring, J.S., Sandström, M.H., Norén, K., Persson, P., 2009. Rethinking arsenate coordination at the surface of goethite. Chem. Eur. J. 15, 5063-5072.

Manceau, A., 1995. The mechanism of anion adsorption on iron oxides: Evidence for the bonding of arsenate tetrahedra on free $Fe(O, OH)_6$ edges. Geochim. Cosmochim. Acta 59, 3647–3653.

Manning, B., 2005. Arsenic speciation in As(III)- and As(V)-treated soil using XANES spectroscopy. Microchim. Acta 151, 181-188.

Manning, B.A., Goldberg, S., 1996. Modeling competitive adsorption of arsenate with phosphate and molybdate on oxide minerals. Soil Sci. Soc. Am. J. 60, 121-131.

Mench, M., Bes, C., 2009. Assessment of ecotoxicity of topsoils from a wood treatment Site. Pedosphere 19, 143-155.

Mench, M., Galende, M., Marchand, L., Kechit, F., Carrier, M., Loppinet-Serani, A., Caille, N., Zhao, F.J., Vangronsveld, J., 2014. Arsenic phytoextraction by *Pteris vittata L*. and frond conversion by solvolysis, In: Litter, M.I., Nicolli, H.B., Meichtry, M., Quici, N., Bundschuh,

J., Bhattacharya, P., Naidu, K. (Eds). One century of the discovery of arsenicosis in Latin America (1914-2014) As2014. CRC Press, pp. 836-838.

Mench, M., Vangronsveld, J., Beckx, C., Ruttens, A., 2006. Progress in assisted natural remediation of an arsenic contaminated agricultural soil. Environ. Pollut. 144, 51-61.

Mähler, J., Persson, I., 2013. Rapid adsorption of arsenic from aqueous solution by ferrihydrite-coated sand and granular ferric hydroxide. Appl. Geochem. 37, 179-189.

Parfitt, R., Childs, C., 1988. Estimation of forms of Fe and Al-a review, and analysis of contrasting soils by dissolution and Mossbauer methods. Soil Res. 26, 121-144.

Peacock, C.L., Sherman, D.M., 2004. Copper(II) sorption onto goethite, hematite and lepidocrocite: A surface complexation model based on ab initio molecular geometries and EXAFS spectroscopy. Geochim. Cosmochim. Acta 68, 2623-2637.

Persson, I., Persson, P., Sandstrom, M., Ullstrom, A.-S., 2002. Structure of Jahn-Teller distorted solvated copper(ii) ions in solution, and in solids with apparently regular octahedral coordination geometry. J. Chem. Soc., Dalton 7, 1256-1265.

Ravel, B., Newville, M., 2005. ATHENA, ARTEMIS, HEPHAESTUS: data analysis for X-ray absorption spectroscopy using IFEFFIT. J. Synchrotron Rad. 12, 537-541.

Reeuwijk, V., 1995. Procedures for Soil Analyses, Sixth ed, Wageningen, Netherlands.

Scheinost, A.C., Abend, S., Pandya, K.I., Sparks, D.L., 2001. Kinetic controls on Cu and Pb sorption by ferrihydrite. Environ. Sci. Technol. 35, 1090-1096.

Sherman, D.M., Randall, S.R., 2003. Surface complexation of arsenic(V) to iron(III) (hydr)oxides: structural mechanism from ab initio molecular geometries and EXAFS spectroscopy. Geochim. Cosmochim. Acta 67, 4223-4230.

Strawn, D.G., Baker, L.L., 2009. Molecular characterization of copper in soils using X-ray absorption spectroscopy. Environ. Pollut. 157, 2813-2821.

Tiberg, C., Sjöstedt, C., Persson, I., Gustafsson, J.P., 2013. Phosphate effects on copper(II) and lead(II) sorption to ferrihydrite. Geochim. Cosmochim. Acta 120, 140-157.

Violante, A., Pigna, M., 2002. Competitive sorption of arsenate and phosphate on different clay minerals and soils. Soil Sci. Soc. Am. J. 66, 1788-1796.

Vu, H.P., Shaw, S., Brinza, L., Benning, L.G., 2013. Partitioning of Pb(II) during goethite and hematite crystallization: Implications for Pb transport in natural systems. Appl. Geochem. 39, 119-128.

Xiao, F., Wang, S., Xu, L., Wang, Y., Yuan, Z., Jia, Y., 2015. Adsorption of monothioarsenate on amorphous aluminum hydroxide under anaerobic conditions. Chem. Geol. 407–408, 46-53.

Xu, Y., Zhou, G.-P., Zheng, X.-F., 2007. Redetermination of iron(III) arsenate dihydrate. Acta Crystallographica Section E 63, i67-i69.

Zabinsky, S.I., Rehr, J.J., Ankudinov, A., Albers, R.C., Eller, M.J., 1995. Multiple-scattering calculations of x-ray-absorption spectra. Phys. Rev. B 52, 2995-3009.

Supplementary material

Immobilization of Cu and As in two contaminated soils with zero-valent iron – Long-term performance and mechanisms

Tiberg, C., Kumpiene, J., Gustafsson, J.P., Marsz, A., Persson, I., Mench, M. and Kleja, D.B.

Table of Contents

Tabel S1

Surface complexation reactions and constants used in the CD-MUSIC model for ferrihydrite and assumed to be valid also for aluminium hydroxide.

Reaction	$(\Delta z_0, \Delta z_1, \Delta z_2)$[a]	log K[b]	Data source(s)
$FeOH^{½-} + H^+ \leftrightarrow FeOH_2^{½+}$	(1,0,0)	8.1	Dzombak & Morel (1990)
$Fe_3O^{½-} + H^+ \leftrightarrow Fe_3OH^{½+}$	(1,0,0)	8.1	Assumed the same as above
$FeOH^{½-} + Na^+ \leftrightarrow FeOHNa^{½+}$	(0,1,0)	-0.6	Hiemstra & van Riemsdijk (2006)
$Fe_3O^{½-} + Na^+ \leftrightarrow Fe_3ONa^{½+}$	(0,1,0)	-0.6	”
$FeOH^{½-} + H^+ + NO_3^- \leftrightarrow FeOH_2NO_3^{½-}$	(1,-1,0)	7.42	”
$Fe_3O^{½-} + H^+ + NO_3^- \leftrightarrow Fe_3OHNO_3^{½-}$	(1,-1,0)	7.42	”
$2FeOH^{½-} + 2H^+ + AsO_4^{3-} \leftrightarrow Fe_2O_2AsO_2^{2-} + 2H_2O$	(0.47,-1.47,0)	27.36	Gustafsson (unpublished)[c]
$2FeOH^{½-} + 3H^+ + AsO_4^{3-} \leftrightarrow Fe_2O_2AsOOH^- + 2H_2O$	(0.58,-0.58,0)	32.42	”
$FeOH^{½-} + 3H^+ + AsO_4^{3-} \leftrightarrow FeOAsO_3H_2^{½-} + H_2O$	(0.5,-0.5,0)	29.50	”
$2FeOH^{½-} + 2H^+ + PO_4^{3-} \leftrightarrow Fe_2O_2PO_2^{2-} + 2H_2O$	(0.46,-1.46,0)	27.59	Tiberg et al. (2013)
$2FeOH^{½-} + 3H^+ + PO_4^{3-} \leftrightarrow Fe_2O_2POOH^- + 2H_2O$	(0.63,-0.63,0)	32.89	”
$FeOH^{½-} + 3H^+ + PO_4^{3-} \leftrightarrow FeOPO_3H_2^{½-} + H_2O$	(0.5,-0.5,0)	30.23	”
$2FeOH^{½-} + Cu^{2+} + H_2O \leftrightarrow (FeOH)_2CuOH + H^+$	(0.5,0.5,0)	0.97	”
$2FeOH^{½-} + 2H^+ + Cu^{2+} + PO_4^{3-} \leftrightarrow (FeO)_2HCuPO_3H^0 + H_2O$	(0.7,0.3,0)	31.71	”

[a] The change of charge in the *o*-, *b*- and *d*-planes respectively.

[b] Two or three numbers indicate binding to sites with different affinity, the percentages of which are within brackets (c.f. text).

[c] Calculated using the data sets treated by Gustafsson and Bhattacharya (2007), but with the updated CD-MUSIC model of Tiberg et al. (2013).

Tabel S2

Cation complexation reactions to soil organic matter in the Stockholm Humic Model (SHM)[a]

Reaction	(Δz_0, Δz_1)[b]	log K	ΔLK_2
$ROH + Cu^{2+} \leftrightarrow ROCu^{+} + H^{+}$	(0.5,0.5)	-1.55	1.4
$2ROH + Cu^{2+} \leftrightarrow (RO)_2Cu + 2H^{+}$	(-0.5,0.5)	-6.0	1.4
$2ROH + Cu^{2+} + H_2O \leftrightarrow (RO)_2CuOH + 3H^{+}$	(-0.5,-0.5)	-13.6	1.4
$2ROH + Al^{3+} \leftrightarrow (RO)_2Al^{+} + 2H^{+}$	(-0.2,1.2)	-4.06	1.06
$2ROH + Al^{3+} + H_2O \leftrightarrow (RO)_2AlOH + 3H^{+}$	(-0.2,0.2)	-9.45	1.06
$ROH + Ca^{2+} \leftrightarrow ROCa^{+} + H^{+}$	(-0.5,1.5)	-2.2	0.3
$2ROH + Fe^{3+} \leftrightarrow (RO)_2Fe^{+} + 2H^{+}$	(-0.2,1.2)	-1.68	1.7
$2ROH + Fe^{3+} + H_2O \leftrightarrow (RO)_2FeOH + 3H^{+}$	(-0.2,0.2)	-4.6	1.7
$ROH + Mg^{2+} \leftrightarrow ROMg^{+} + H^{+}$	(-0.5,1.5)	-2.5	0.3

[a]Reactions for Cu^{2+} is from Linde et al. (Water Air Soil Pollut. 183, 69-83, 2007), those for Al^{3+} are from Gustafsson et al. (2011), those for $Ca^{2+}$and Mg^{2+} are from Gustafsson et al. (Environ. Sci. Technol. 41, 1232-1237, 2007), and those for Fe^{3+} are from Sjöstedt et al. (Geochim. Cosmochim. Acta 105, 172-186, 2013).

[b]The change of charge in the *o*- and *d*-planes respectively.

Table S3

Geochemically active concentrations used in geochemical modeling.

	Al[a] (mg L^{-1})	Ca[b] (mg L^{-1})	Cu[b] (mg L^{-1})	Fe[a] (mg L^{-1})	K[b] (mg L^{-1})	Mg[b] (mg L^{-1})	As[a] (mg L^{-1})
CuUNT	63	33	35	39	120	3.7	0.78
CuZVI	34	39	65	120	5.2	4.8	1.4
AsUNT	113	158	1.6	71	7.8	32	9.1
AsZVI	107	165	2.1	161	6.7	38	10

[a] Extracted with 0.2 mol L^{-1} oxalate/oxalic buffer at pH 3.

[b] Extracted with 0.1 mol L^{-1} HNO_3

Table S4

Ranges of pH, DOC, phosphate and Fh model entries.

	pH	DOC[a] (mg L^{-1})	$PO_4^{-3,a}$ (mg L^{-1})	Fh[b] (g L^{-1})
CuUNT	3.2-9.0	3.1-94	0.01-0.98	0.14-0.37
CuZVI	2.9-8.5	2.8-25	0.01-0.22	2.49-2.66
AsUNT	4.6-8.1	11-21	2.2-2.9	0.43-0.53
AsZVI	4.9-8.0	5.8-14	0.06-0.98	0.96-1.01

[a] Interpolated between measured concentrations in the supernatant after equilibration.

[b] Solid concentration of adsorbing iron/aluminum (hydr)oxides in the CD-MUSIC model, parameterized as ferrihydrite. The sum of oxalate-extractable iron and aluminum was recalculated to solid concentration of sorbent.

Table S5

Dissolved concentrations in batch experiments with the copper-contaminated soils, mean values of duplicates (+/- range).

	pH	Al	Ca	Fe	K	Mg	Cu	DOC
		µmol L^{-1}	µmol L^{-1}	µmol L^{-1}	µmol L^{-1}	µmol L^{-1}	µmol L^{-1}	mg L^{-1}
CuUNT	3.29 (0.03)	838 (33)	706 (32)	10 (2.0)	99 (8.4)	125 (5.8)	378 (44)	5.5 (0.1)
	3.98 (0.12)	93 (13)	598 (11)	1.6 (0.3)	81 (1.8)	114 (8.2)	188 (18)	3.1 (0.0)
	6.01 (0.01)	1.7 (0.1)	179 (0.5)	0.8 (0.1)	52 (31)	42.4 (0.0)	5.2 (0.5)	5.9 (0.3)
	8.04 (0.01)	86 (37)	55 (1.2)	85 (27)	37 (2.4)	9.8 (0.2)	21 (3.9)	43 (0.9)
	8.98 (0.09)	99 (18)	70 (1.5)	45 (5.5)	34 (2.3)	9.0 (0.3)	48 (2.1)	94 (2.7)
CuZVI	2.98 (0.04)	718 (20)	7945 (61)	520 (64)	121 (3.3)	155 (2.9)	759 (16)	3.5 (0.2)
	3.97 (0.03)	228 (20)	754 (5.0)	190 (9.0)	115 (1.3)	144 (2.4)	560 (71)	3.3 (0.3)
	6.59 (0.02)	0.3 (0.1)	165 (0.6)	0.3 (0.0)	62 (0.0)	48 (0.6)	1.5 (0.0)	2.7 (0.4)
	8.09 (0.04)	23.5 (4.8)	36 (1.5)	110 (23)	51 (1.4)	8.8 (0.3)	13 (1.6)	23 (3.1)
	8.45 (0.05)	34.8 (2.7)	38 (1.5)	146 (4.4)	73 (12)	8.5 (0.5)	18 (0.9)	24 (2.9)

Table S6

Dissolved concentrations in batch experiments with the arsenic-contaminated soils, mean values of duplicates (+/- range).

	pH	Al	Ca	Fe	K	Mg	As	DOC
		µmol L^{-1}	µmol L^{-1}	µmol L^{-1}	µmol L^{-1}	µmol L^{-1}	µmol L^{-1}	mg L^{-1}
AsUNT	4.74 (0.07)	76 (7.0)	2657 (62)	1.3 (0.1)	124 (2.4)	1096 (43)	8.3 (1.1)	11 (0.4)
	5.14 (0.04)	39 (1.7)	2251 (22)	1.2 (0.0)	118 (1.3)	997 (10)	6.2 (0.1)	11 (0.5)
	6.15 (0.02)	8.1 (0.0)	1543 (16)	1.3 (0.2)	106 (9.0)	804 (6.2)	4.4 (0.3)	12 (0.4)
	7.79 (0.03)	7.0 (0.7)	425 (6.2)	4.9 (1.0)	91 (4.7)	280 (1.9)	3.9 (0.1)	16 (0.1)
	8.05 (0.03)	20 (1.3)	317 (12)	12 (0.5)	91 (12)	206 (8.8)	5.5 (0.2)	21 (0.1)
AsZVI	5.02 (0.15)	73 (8.7)	2657 (12)	3.1 (0.8)	99 (4.5)	1133 (6.2)	0.5 (0.0)	5.8 (0.15)
	5.53 (0.04)	25 (1.4)	2349 (1.2)	5.0 (2.4)	105 (5.8)	1158 (14)	0.4 (0.1)	6.0 (0.26)
	6.12 (0.12)	7.2 (1.3)	1859 (17)	2.7 (0.6)	95 (1.3)	1010 (2.1)	0.5 (0.2)	6.9 (0.57)
	6.91 (0.03)	2.7 (0.1)	1109 (6.2)	5.0 (0.2)	100 (4.0)	701 (6.2)	0.9 (0.1)	9.9 (0.22)
	7.95 (0.00)	3.3 (0.1)	434 (10)	2.0 (0.7)	76 (2.1)	314 (7.8)	2.1 (0.0)	13.5 (0.19)

Table S7

Preparation of standards for XAS measurements. All samples were prepared with a background electrolyte of 10 mmol L^{-1} $NaNO_3$.

Cu-fulvic acid	Solution containing 3 mmol L^{-1} copper and 8 g L^{-1} Suwannee River Fulvic Acid (processed by the International Humic Substances Society, IHSS).
Cu or As to ferrihydrite	The copper sample was prepared and measured by Tiberg et al. (2013). The arsenic sample was prepared in the same way; Batches of 0.3 mmol L^{-1} laboratory synthesized ferrihydrite (Tiberg et al., 2013) and 30 µmol L^{-1} As equilibrated for 24 h. XAS measurement on wet ferrihydrite paste after centrifugation.
Cu or As to aluminum hydroxide	Samples for sorption on amorphous aluminum hydroxide were prepared in batches containing 1 mmol L^{-1} aluminum hydroxide + 50 µmol L^{-1} copper or 1 mmol L^{-1} aluminum hydroxide + 100 µmol L^{-1} arsenate. Samples were equilibrated for 24 h, centrifuged and measurements were made on wet paste. Preparation of aluminum hydroxide is described below.

Preparation of amorphous aluminum hydroxide: A solution containing 36 mmol L^{-1} $Al(NO_3)_3$ and 12 mmol L^{-1} $NaNO_3$ was brought to pH 7.0 through drop-wise addition of 4 mol L^{-1} NaOH (prepared just before it was used). The resulting suspension was aged for about 16 h at 20^{o}C. After ageing the aluminum hydroxide suspension was back-titrated with 0.1 mol L^{-1} HNO_3 to pH 5 and stirred for about 30 min before preparation of batches with copper or arsenic to avoid the presence of excessive CO_2 in the suspensions.

XAS measurements: All copper measurements were made with a Ni filter placed between the sample and fluorescence detector and internal energy calibration was made with a foil of metallic copper assigned to 8,979 eV(Thompson et al., 2009). All arsenic measurements were made using a Ge filter and internal calibration with an As foil assigned to 11,867 eV (Thompson et al., 2009).

X-ray absorption spectroscopy, MAX-Lab, Sweden: Beam line I811 operated at 1.5 GeV with a maximum ring current of 400 mA and electrons were refilled twice a day. The end-station was equipped with a Si[111] double crystal monochromator. The measurements were performed in fluorescence mode using a PIPS detector. During copper measurements the monochromator was detuned 50% of maximum intensity to reduce higher-order harmonics. The measurements were performed in 2013 with 10 scans for CuUNT and 6 scans for CuZVI. For the arsenate sorbed to ferrihydrite standard spectrum, 5 scans at 20% detuning were collected with a Ge filter in September 2014 and for arsenate sorbed to aluminum hydroxide 6 scans at 20% detuning were collected in May 2015.

X-ray absorption spectroscopy, Stanford Synchrotron Radiation Lightsource (SSRL), US: Beam line 4-1 operated at 3.0 GeV and with a maximum ring current of 500 mA (top-up mode). The station was equipped with a Si[220] double crystal monochromator detuned 50-65% of maximum intensity. The measurements were performed in fluorescence mode using a Lytle detector. For soil samples, 7 scans each were collected and for sorption of copper to aluminum hydroxides or fulvic acid 4-5 scans. All spectra were collected in February 2014 except the Cu-ferrihydrite spectra that was previously published. Details about that can be found in Tiberg et al. (2013).

Table S8

Model entries for scenario simulations

Parameter	Value
pH	4-9
Cu, "available concentration" (mmol L^{-1})	1
Al, Ca, Fe, K, Mg, As, "available concentration"	Values for CuUNT, Table S1
DOC, PO_4^{3-}	Values for CuUNT Table S2
Na, NO_3^- (mmol L^{-1})	10
Sorbent; Fh (g L^{-1})	UNT; 0.14-0.37 +1% ZVI; 1.35-1.55 +2% ZVI; 2.53-2.73
SOM; FA and HA (g L^{-1})	0.5% org-C; 0.25 2% org-C: 1

Wavelet transforms (WT): WT reveal if the back-scattering that give rise to the peaks in the FT comes from heavy or light atoms. Wavelet transforms were made at *R*-range 2-4 Å with parameters κ = 7 (Cu) or 6 (As) and σ = 1. The results are presented in three-dimensional plots with the photoelectron wavenumber (*k*) on the x-axis, interatomic distance (*R*) on the y-axis (not corrected for phase shift) and the WT modulus at the y-axis, forming ridges that help to locate back-scatterers. White/brown areas indicate high intensity of the WT modulus whereas blue/green areas indicate low intensity. High intensity of WT modulus at k >6 implies presence of heavy back-scatterers like iron. Below $R+\Delta R$ = 2.3 Å the high intensity is contributions from Cu-O or As-O distances at all *k*.

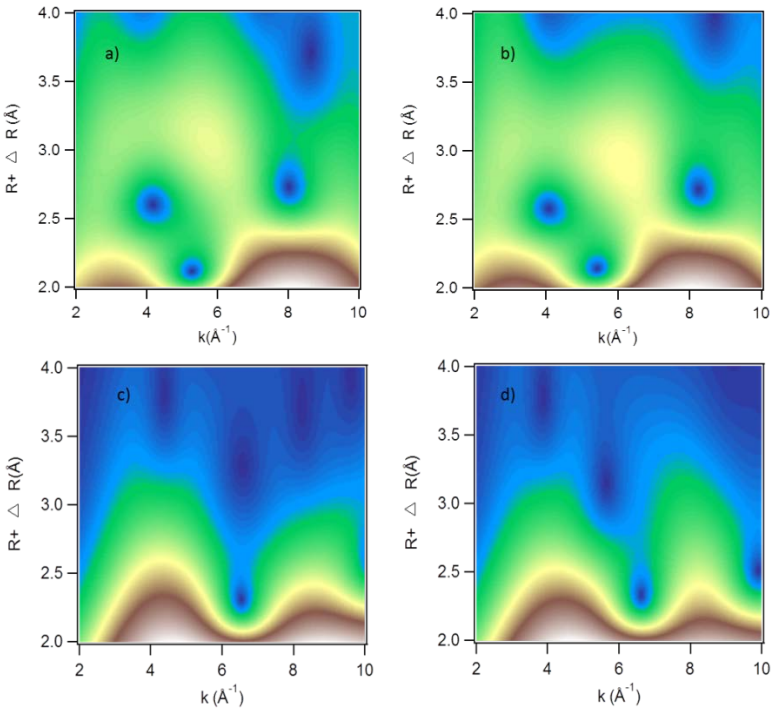

Fig S1. WT analysis of copper standard spectra and models; a) Cu-fulvic acid, WT of measured spectra, b) Cu-fulvic acid, WT model fit, *k*-range 2.7-9.5 Å^{-1}. c) Cu-Alhydroxide, WT of measured spectra, d) Cu-Alhydroxide WT model fit, *k*-range 3-12 Å^{-1}.

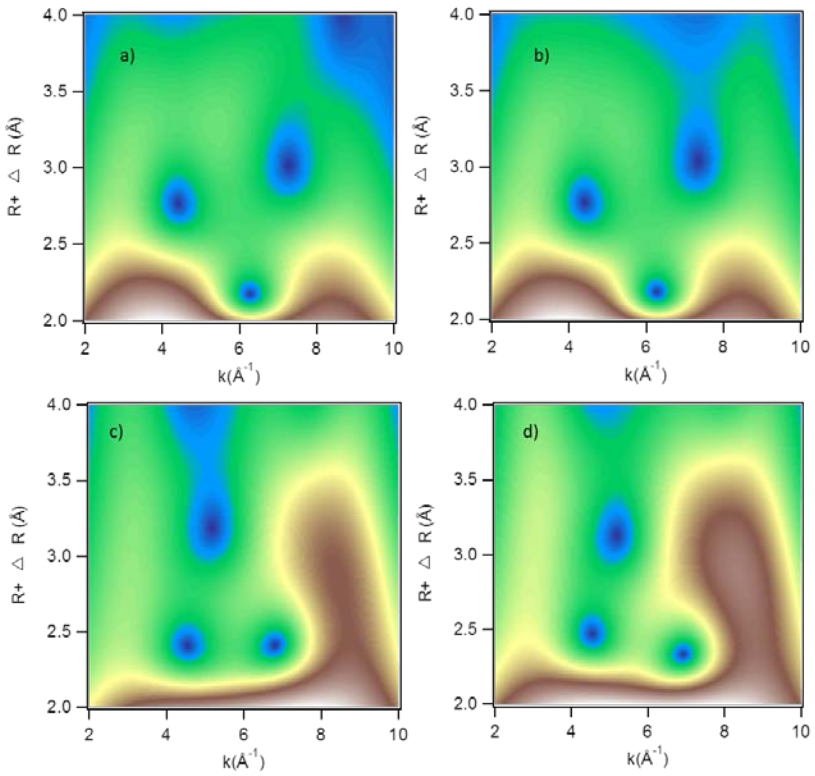

Fig S2. WT analysis of Cu contaminated soils and models; a) CuUNT, WT of measured spectra, b) CuUNT, WT of best model fit, c) CuZVI, WT of measured spectra, d) CuZVI, WT of best model fit. K-range 2.9-9 Å^{-1} (CuUNT), 3-9 Å^{-1} (CuZVI).

WT of spectra for Cu-fulvic acid (Figure S1a) or CuUNT (Figure S2a) indicated no presence of heavy back-scatterers. Heavy back-scatterers were indicated in the WT of CuZVI (Figure S2c) and Cu-ferrihydrite (WT in Tiberg et al.(2013)) expressed as high intensity of the WT modulus at k = 8-9 Å^{-1} and $R+\Delta R$ = 2.5-3.5 Å (about 3-4 Å phase shifted). There was a small increase in the WT modulus at k = 5 and $R+\Delta R$ = 2.3-2.5 (about 2.8-3 Å phase shifted) in WT of spectra for Cu-Alhydroxide (Figure S1c) that might come from Al back-scattering.

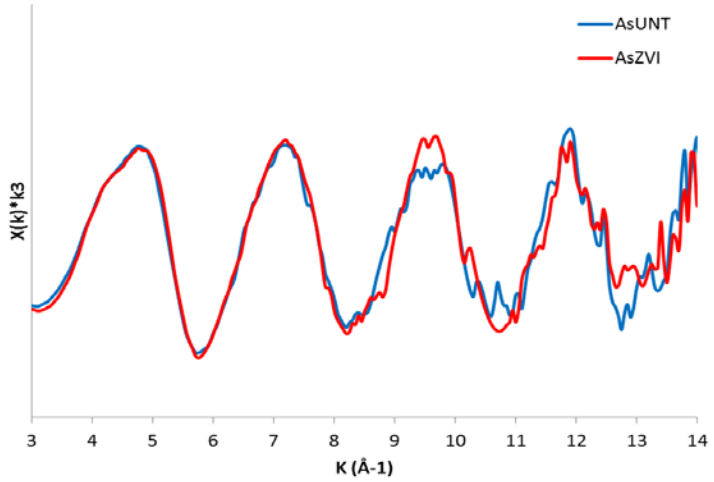

Fig S3. Superimposed EXAFS spectra of AsUNT and AsZVI.

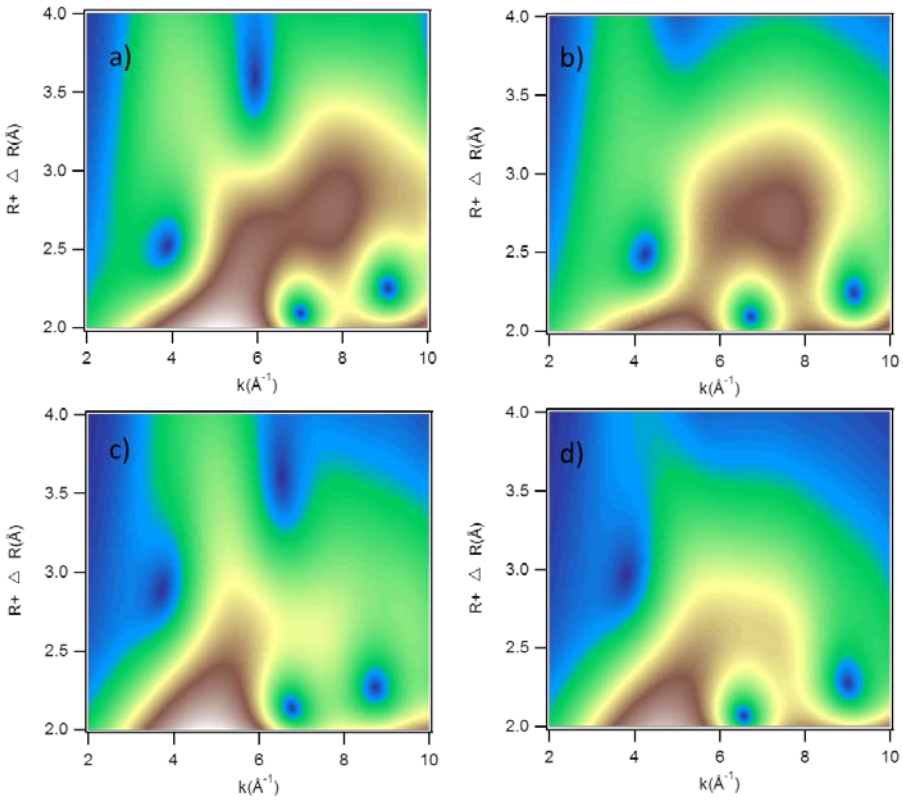

Fig S4. WT analysis of arsenate standard spectra; a) WT of measured As-ferrihydrite spectra, b) WT of model fit, c) WT of measured As-Alhydroxide spectra, d) WT of model fit. The *k*-ranges used were 3.6-12.4 $Å^{-1}$ (As-ferrihydrite) and 3.9-13 $Å^{-1}$ (As-Alhydroxide).

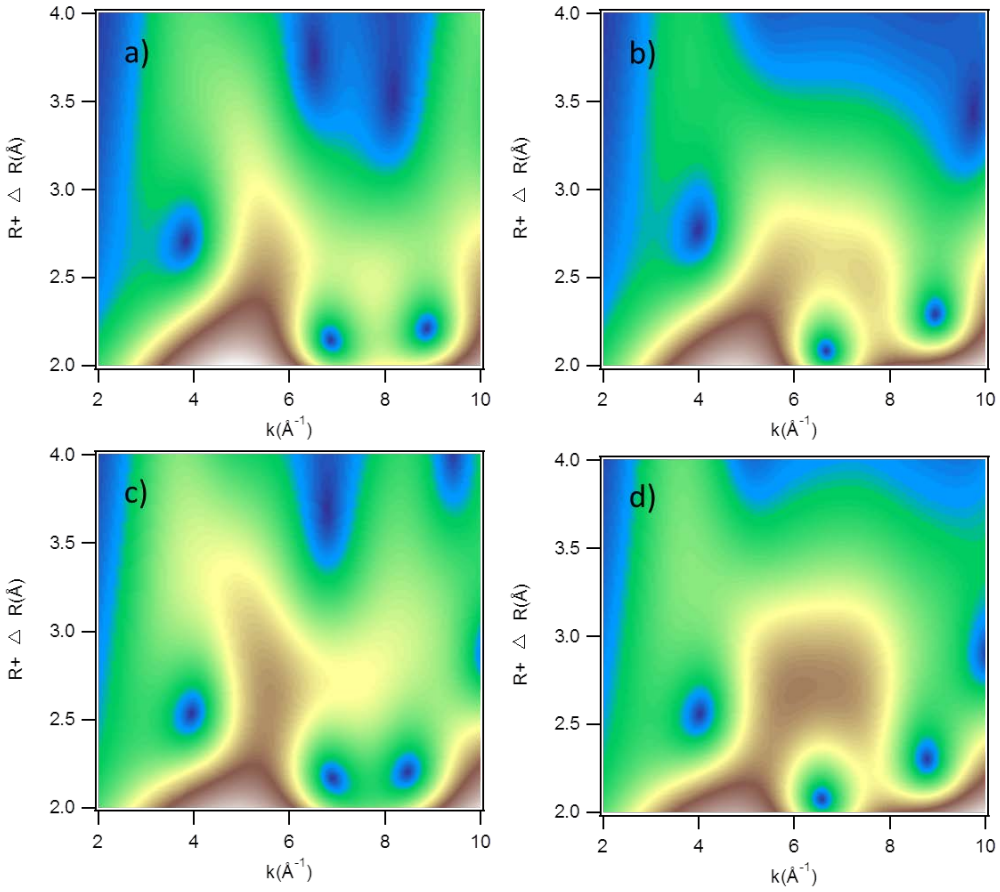

Fig S5. WT analysis of arsenic contaminated soils and models; a) AsUNT, WT of measured spectra, b) AsUNT, WT of model fit, c) AsZVI, WT of measured spectra, d) AsZVI, WT of model fit. The *k*-range was 2.8-11 Å^{-1} for both samples.

In the WT of arsenic spectra there are indications of back-scatterers in all plots (Figure S4 and S5). The intensity of the WT modulus is increased at k = 5-8 and $R+\Delta R$ = 2.5-3.2 Å (about 3.0-3.7 Å phase shifted) for the As-ferrihydrite spectrum, k = 5-6 Å^{-1} and $R+\Delta R$ = 2.3-2.8 Å (about 2.8-3.3 Å phase shifted) for the As-Alhydroxide spectrum, $R+\Delta R$ = 2.3-3.0 Å (about 2.8-3.5 Å phase shifted) for the AsUNT spectrum and $R+\Delta R$ = 2.3-3.2 Å (about 2.8-3.7 Å phase shifted) for the AsZVI spectrum.

Table S9

Summary of copper and arsenic K-edge EXAFS shell fit results[a]. Parameters in italics were constrained during fitting.

Sample	Path	CN	R (Å)	σ^2 (Å^2)	ΔE (eV)	S_0^2	R-factor (%)
CuUNT	Cu–O	*4*	1.93 (0.01)	0.006 (0.000)	4.78 (0.61)	*0.7*	0.1
pH=6.00	Cu···C	*4*	2.76 (0.02)	0.010 (0.003)			
	Cu···C–O	*8*	2.97 (0.03)	0.020 (0.006)			
	Cu–O–O	*12*	3.86 (0.02)	0.005 (0.003)	*k*-range used: 2,9-9 Å^{-1}		
CuZVI	Cu–O	*4*	1.97 (0.01)	0.004 (0.000)	-1.18 (1.42)	*0.7*	1.2
pH=6.47	Cu···Fe1	*1*	3.09 (0.04)	0.009 (0.005)			
	Cu···Fe2	*1*	3.89 (0.05)	0.004 (0.006)	*k*-range used: 3-9 Å^{-1}		
Cu-Fulvic acid	Cu–O	*4*	1.94 (0.01)	0.004 (0.001)	-2.76 (1.44)	*0.8*	0.7
pH=4.77	Cu···C	*4*	2.85 (0.05)	0.008 (0.006)			
	Cu···C–O	*8*	3.05 (0.09)	0.018 (0.013)			
	Cu···O2	*4*	3.73 (0.04)	0.006 (0.005)	*k*-range used: 2.7-9.5 Å^{-1}		
Cu-Ferrihydrite[b]	Cu–O	*4*	1.94 (0.01)	0.005 (0.000)	-0.96 (0.64)	*0.8*	0.6
pH=5.85	Cu···Fe1	*1*	3.02 (0.02)	0.007 (0.002)			
	Cu–O–O	*12*	3.88 (0.02)	0.005 (0.004)	*k*-range used: 2.7-10.5 Å^{-1}		
Cu-Alhydroxide	Cu–O	*4*	1.96 (0.01)	0.005 (0.000)	-4.22 (0.84)	*0.8*	0.8
pH=5.92	Cu···Al1	*1*	2.97(0.02)	0.007(0.028)			
	Cu–O–O	*12*	4.02 (0.05)	0.015 (0.008)	*k*-range used: 3.0-12 Å^{-1}		
AsUNT	As–O	*4*	1.70 (0.01)	0.002 (0.000)	3.19 (1.54)	*1.0*	1.0
pH=7.79	As–O–O	*12*	3.09 (0.06)	*0.002*			
	As···Al	*2*	3.19 (0.06)	0.010 (0.006)	*k*-range used: 3.6-11 Å^{-1}		
AsZVI	As–O	*4*	1.69 (0.01)	0.001 (0.000)	1.78 (1.59)	*1.0*	0.9
pH=7.95	As–O–O	*12*	3.06 (0.06)	*0.001*			
	As···Al	*1*	3.19 (0.09)	0.003 (0.012)			
	As···Fe	*1*	3.39 (0.08)	0.008 (0.009)	*k*-range used: 3.5-11.2 Å^{-1}		
As-Ferrihydrite	As–O	*4*	1.69 (0.00)	0.002 (0.000)	0.43 (1.16)	*1.0*	1.0
pH=7.18	As–O–O	*12*	3.08 (0.03)	*0.002*			
	As···Fe	*2*	3.31 (0.02)	0.010 (0.002)	*k*-range used: 3.6-12.4 Å^{-1}		
As-Alhydroxide	As–O	*4*	1.70 (0.00)	0.002 (0.000)	0.23 (1.31)	*1.0*	0.4
pH=6.26	As–O–O	*12*	3.10 (0.05)	*0.002*			
	As···Al	*2*	3.21 (0.04)	0.009 (0.005)	*k*-range used: 3.9-13 Å^{-1}		

[a] CN = Coordination number; R = Atomic distance; σ2 = Debye-Waller factor; ΔE = Energy shift parameter; S_0^2 = Passive amplitude reduction factor; R-factor = goodness-of-fit parameter of the Fourier Transform; sum of the squares of the differences between the data and the fit at each data point, divided by the sum of the squares of the data at each corresponding point. In general, R-factor values < 5% reflect a reasonable fit. Uncertainties of fitted parameters as given in Artemis (Ravel and Newville, 2005).

[b] Previously published by Tiberg et al. (2013).

EXAFS model fit results: Besides the Cu···C distance at about 2.8 Å and the Cu···C–O distance at about 3 Å, the model fit for the Cu-fulvic acid sample includes a second copper-oxygen distance, Cu···O2 at 3.73 Å, also typical for a chelate ring (Karlsson et al., 2006). The spectrum for CuUNT was best fit by addition of another multiple scattering path: Cu–O–O at 3.86 Å (180˚ multiple scattering within the CuO_6 octahedron).

A Cu···Al distance of about 3.0 Å is consistent with an edge-sharing or a monodentate complex on the Al hydroxide surface (Cheah et al., 1998). Meaningful EXAFS models for CuZVI were not obtained with Cu···C or Cu···Al distances. CuZVI was best fit with two Cu···Fe distances. The shorter Cu···Fe distance is consistent with a combination of inner-sphere complexes on ferrihydrite and goethite/hematite. Edge-sharing complexes on ferrihydrite with Cu···Fe ~3.0 Å (Scheinost et al., 2001; Tiberg et al., 2013) and edge-sharing or corner-sharing complexes on goethite with Cu···Fe ~3.14-3.21 Å (Alcacio et al., 2001; Peacock and Sherman, 2004). EXAFS cannot separate distances this close. The longer Cu···Fe distance could be consistent with a monodentate association to the iron (hydr)oxide surface (Cu–O ~1.9 Å + Fe–O ~2.0 Å), possibly bonding to the surface also via another ion or humic acid in a ternary complex. There are evidence for ternary copper complexes on iron (hydr)oxide surfaces (Song et al., 2008; Swedlund and Webster, 2001; Tiberg et al., 2013) and WT of a model including a Cu···Fe at ~3.9 Å matched the WT of the CuZVI spectra more closely (Figure S3c, S3d) than a WT of model without this distance (not shown). If the third participant in a ternary complex is a light element (for example carbon) this element would not be easily distinguishable by EXAFS.

Multiple scattering within the arsenate tetrahedron, As–O–O at ~3.1 Å (Table S6) had to be included in all model spectra of arsenic samples.

References

Alcacio, T.E., Hesterberg, D., Chou, J.W., Martin, J.D., Beauchemin, S., Sayers, D.E., 2001. Molecular scale characteristics of Cu(II) bonding in goethite–humate complexes. Geochim. Cosmochim. Acta 65, 1355-1366.

Cheah, S.-F., Brown, G.E., Parks, G.A., 1998. XAFS spectroscopy study of Cu(II) sorption on amorphous SiO_2 and γ-Al_2 O_3: Effect of substrate and time on sorption complexes. J. Colloid Interface Sci. 208, 110-128.

Karlsson, T., Persson, P., Skyllberg, U., 2006. Complexation of copper(II) in organic soils and in dissolved organic matter − EXAFS evidence for chelate ring structures. Environ. Sci. Technol. 40, 2623-2628.

Peacock, C.L., Sherman, D.M., 2004. Copper(II) sorption onto goethite, hematite and lepidocrocite: A surface complexation model based on ab initio molecular geometries and EXAFS spectroscopy. Geochim. Cosmochim. Acta 68, 2623-2637.

Ravel, B., Newville, M., 2005. ATHENA, ARTEMIS, HEPHAESTUS: data analysis for X-ray absorption spectroscopy using IFEFFIT. J. Synchrotron Rad. 12, 537-541.

Scheinost, A.C., Abend, S., Pandya, K.I., Sparks, D.L., 2001. Kinetic controls on Cu and Pb sorption by ferrihydrite. Environ. Sci. Technol. 35, 1090-1096.

Song, Y., Swedlund, P.J., Singhal, N., 2008. Copper(II) and cadmium(II) sorption onto ferrihydrite in the presence of phthalic acid: Some properties of the ternary complex. Environ. Sci. Technol. 42, 4008-4013.

Swedlund, P.J., Webster, J.G., 2001. Cu and Zn ternary surface complex formation with SO4 on ferrihydrite and schwertmannite. Appl. Geochem. 16, 503-511.

Thompson, A., Attwood, D., Gullikson, E., Howells, M., Kim, K.-J., Kirtz, J., Kortright, J., Lindau, I., Liu, Y., Pianetta, P., Robinson, A., Scofield, J., Underwood, J., Williams, G., Winck, H., 2009. X-ray Data Booklet. Lawrence Berkeley National Laboratory, University of California, Berkeley, California.

Tiberg, C., Sjöstedt, C., Persson, I., Gustafsson, J.P., 2013. Phosphate effects on copper(II) and lead(II) sorption to ferrihydrite. Geochim. Cosmochim. Acta 120, 140-157.